Design and analysis of a new scheme of the FOSTA for DFIG based wind turbine

Kheira Belgacem, Houaria Abdelli, Mebarka Atig, Abdelkader Mezouar
Laboratory of Electro-Technical Engineering, Department of Electrotechnics and Automation, Faculty of Science and Technology, Tahar Moulay University of Saida, Saida, Algeria

Article Info

Article history:

Received May 19, 2025
Revised Sep 17, 2025
Accepted Oct 19, 2025

Keywords:

Active and reactive power
Doubly fed induction generator
Fractional calculus theory
Super twisting algorithm
Wind turbine

ABSTRACT

An super-twisting algorithm (STA)-based controller was designed and implemented in this study to achieve precise control over the stator active and reactive power of a doubly fed induction generator (DFIG)-equipped wind turbine device. The fractional calculus theory (FCT) allowed the STA to maximize its effectiveness and performance. A distinct form is sent to the FCT-based STA controller. The stator flux orientation technique uses control that is independent of stator active and reactive powers. In order to achieve a quick system with sufficient precision and a robust control strategy, the hybrid method control is based on the fractional-order super twisting algorithm (FOSTA) and FCT. To demonstrate the performance, efficacy, and resilience of the stated nonlinear approach, a number of simulations are provided.

Corresponding Author:

Kheira Belgacem
Laboratory of Electro-Technical Engineering, Department of Electrotechnics and Automation
Faculty of Science and Technology, Tahar Moulay University of Saida
B.P. 138, 20000, Ennasr, Saida, Algeria
Email: kheira.belgacem@yahoo.fr

1. INTRODUCTION

Significant electrical energy is needed for technological advancement and the enhancement of human life, yet this energy's production and consumption directly contributes to the exacerbation of environmental issues, including air pollution, global warming, and increased carbon dioxide emissions, among other negative impacts [1]. We employ clean, renewable energy sources, including wind energy, to reduce these issues; changing the kinetic the process of turning wind energy into electrical power involves two phases: at the turbine's (rotor's) level, which transforms a portion of the available wind energy into mechanical energy. At the generator's level, mechanical energy is received, transformed into electrical power, and then sent to the electrical network. An electromechanical device uses the wind to generate energy [2].

The most popular method of producing electricity is technology for wind turbines with variable speeds, which is based on a doubly fed induction generator (DFIG). Currently, the wind's varied speed system based on the DFIG is the most commonly used in onshore wind farms. Its major advantage lies in the fact that its static converters in three phases are designed for a fraction of the DFIG's nominal power, which represents a significant economic advantage over other electromechanical conversion options [3].

Indirect field-oriented control (IFOC) known as vector control, is an independent control technique particularly applied to the control of alternating current (AC) machines. Vector control using conventional regulators (proportional, integral, and derivative) is not always able to effectively manage transient conditions and, in general, variations in machine parameters. However, other types of control, such as synergetic control or artificial intelligence, are better suited to these requirements and offer greater sensitivity and robustness [4].

Because wind energy generation is so important, strong controls the system is parametric and insensitive to outside perturbations fluctuations have been designed because of research. It is the process of developing strategies with improved performance and optimizing the energy quality in the electrical network by applying scientific approaches and technical techniques. In Herizi *et al*. [5], the proportional-integral (PI) controller was swapped out for a sliding mode control (SMC). As the response time and ripple capabilities dropped, the use of SMC greatly enhanced the characteristics of the control strategy as in contrast to the traditional control approach. In order to maximize the control's effectiveness. Belgacem *et al*. [6] employed yet another clever method. To reduce capacity variations and enhance the quality of the energy produced by the DFIG, fuzzy control was employed as a clever technique. The results of the simulation illustrate the effectiveness of fuzzy control to maximize its advantages. To improve the control strategy's performance, some researchers have suggested replacing nonlinear approaches. Nonlinear techniques are substituted for the PI controller in order to reduce power fluctuations and produce a method that is independent of changes features of the system being examined.

This work builds on the work of Abdelli *et al*. [7], where the PI controller of the conventional control strategy is replaced with the novel fractional-order super twisting algorithm (FOSTA) technique. Additionally, the electrical power, power ripple value and the super-twisting algorithm (STA) reaction time and the indirect FOSTA approach developed in this work are compared. Presenting a fresh idea for the FOSTA controller that improves the contribution of the paper is the quality of the power generated by DFIG

Consequently, the structure of this work. First, the wind turbine system is presented. Models are made for the wind turbine and the DFIG, respectively. The main advantages of this strategy are then described along with an explanation of the new fractional-order nonlinear approach FOSTA. The pertinent information about the intended control strategy for a DFIG is then given. Lastly, a comparison and analysis of the DFIG control strategy's characteristics utilizing fractional-order FOSTA controllers are conducted.

2. THE CONTROL SCHEMA

Both the FOSTA methods and the basic theoretical representations of the super twisting sliding mode control (STSMC) are offered here for controlling the generic stiff system dynamics.

2.1. Super-twisting algorithm control design

This section makes the case that SMC suffers from the chattering phenomena, which is oscillations that happen when the system trajectory crosses the sliding surface, even though it is effective against constrained uncertainties and disturbances [8]. As a remedy, the STA is presented, which considerably lowers chattering while maintaining the robustness of SMC. In contrast to traditional SMC, which requires a sliding variable of the system's order, the STA only requires motion variables of its own order for the same system, which is a significant benefit. The STA is a well-liked option in many engineering fields, such as renewable energy, electronics, and control, because of its affordability, robustness, and ease of use. The precise STA control law mentioned in (1) is cited in the text's conclusion [9].

$$\begin{cases} u_{ST} = u_1 + u_2 \\ \dot{u}_1 = \rightleftarrows -\lambda sign(S) \\ u_2 = -\alpha |s|^{\frac{1}{2}} sign(S) \end{cases} \tag{1}$$

where: $\alpha > 0, \lambda > 0$ the trajectory can converge to the sliding surface under the following conditions [10], [11].

$$\begin{cases} \lambda > \frac{C}{K_m} \\ \alpha^2 \geq \frac{4CK_M(\lambda+C)}{{K_m}^3(\lambda-C)} \end{cases} \tag{2}$$

where the STSMC positive constants are: C,K_M,K_m. The control law consists of two parts (1). However, the second component is a continuous function of the sliding variable; the first part is a continuous function of the sliding variable, while the first component depends on the discontinuous derivative of the sliding variable [12]. Based on (1), Figure 1 shows a simplified representation of the STA controller's operation and was created to facilitate understanding and use of the STA controller.

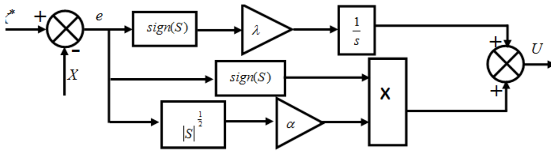

Figure 1. Traditionnal STA controller

Even if the STA works well, fluctuations in both reactive and active power are still present when it is used in automated systems like wind energy generating. Furthermore, the resulting poor current quality can interrupt equipment operation. The fractional-order (FO) approach [13] is suggested as a solution to these problems. The goal of this new nonlinear approach is to increase reliability while maintaining the original STA's simplicity and use.

2.2. Proposed fractional-order super twisting algorithm controller

This paper suggests a novel STA controller model based on the FO to get better the control strategy's performance and efficacy. Fractional calculus is widely recognized as a mathematical technique intended to tackle difficult problems. Because of its benefits over alternative methods, it is utilized in a variety of industries, including renewable energy. The primary benefits of this approach are sustainability and adaptability [14], [15]. The STA controller's simplicity and ease of use are retained in the new controller, which combines fractional calculus with the STA controller.

In addition, the FOSTA controller is an altered STA controller designed to increase longevity. Additionally, the following (3) can be used to determine the mathematical representation of the intended fractional calculus theory (FCT) technique: where $\gamma \neq 0$ [15].

$$\begin{cases} u_{ST} = [u_1 + u_2]^{\gamma} \\ \dot{u}_1 = \rightleftarrows -\lambda sign(S) \\ u_2 = -\alpha |s|^{\frac{1}{2}} sign(S) \end{cases} \quad (3)$$

In Figure 2, the suggested FOSTA controller is shown. The FOSTA technique is simple, easy to implement, and easy to change, as seen in Figure 2. Furthermore, this proposed method is easy to apply to complex systems. In the next section, the constructed nonlinear controller is used to control the DFIG-based wind power.

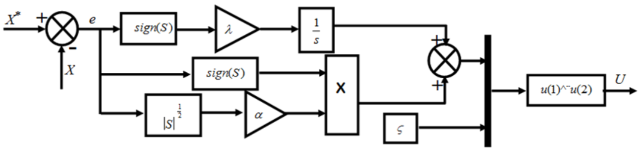

Figure 2. The suggested FOSTA controller

3. WIND TURBINE AND GEARBOX MODELING

The modelling of a wind turbine relies on the conversion of the wind's kinetic energy into mechanical energy, and then into electricity. It is based on the wind power equation [16].

$$P_v = \frac{\rho \cdot S \cdot V^3}{2} \quad (4)$$

The following is an expression for the aerodynamic power that appears at the turbine rotor [17]:

$$P_{aer} = C_p \cdot P_v = C_p(\lambda, \beta) \cdot \frac{\rho \cdot S \cdot V^3}{2} \quad (5)$$

The variable $C_p(\lambda, \beta)$ is the aerodynamic power coefficient. It is dependent on two: the tip speed ratio λ and the orientation angle of the blades (or pitch angle, often denoted by β). The tip speed ratio ratio λ, which is the ratio of the speed of the turbine blade tips. The following statement [18] defines it in relation to wind speed:

$$\lambda = \frac{R\Omega_{turbine}}{v} \tag{6}$$

where: R is the radius of the turbine $\Omega_{turbine}$ is angular speed of the turbine and v is the wind speed. The expression for $C_p(\lambda, \beta)$ is given by [19].

$$C_p(\lambda, \beta) = (0.5 - 0.167 \cdot (\beta - 2)) \cdot sin\left[\frac{\pi.(\lambda+0.1)}{10-0.3.\beta}\right] - 0.00184 \cdot (\lambda - 3) \cdot (\beta - 2) \tag{7}$$

The expression for the aerodynamic power coefficient is generally complex and non-linear, and it varies depending on the specific turbine design [20].

$$T_{aer} = \frac{P_{aer}}{\Omega_{turbine}} = C_p \frac{\rho \cdot S \cdot V^3}{2} \frac{1}{\Omega_{turbine}} \tag{8}$$

4. MODELING OF THE DOUBLY FED INDUCTION GENERATOR

As seen in Figure 3, a wind turbine that uses a DFIG links its stator straight to the power grid. The rotor is connected to a back-to-back power converter via individual slip rings for each winding. The converter only needs to manage a small portion of the total stator power, usually up to 30%, which is a major benefit of the DFIG architecture [21].

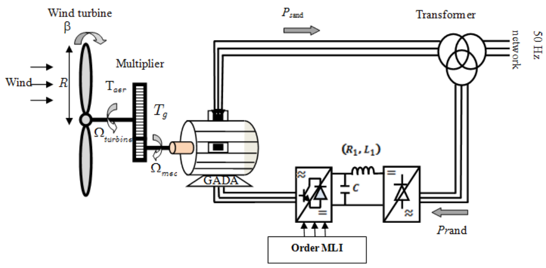

Figure 3. Block schematic of a wind turbine using DFIG

Bekiroglu and Yazar [22] provides a description of the DFIG stator and rotor voltage mathematical model in the park reference frame (d, q):

$$\begin{cases} v_{ds} = R_s i_{ds} + \frac{d}{dt}\varphi_{ds} - \omega_s \varphi_{qs} \\ v_{qs} = R_s i_{qs} + \frac{d}{dt}\varphi_{qs} + \omega_s \varphi_{ds} \end{cases} \tag{9}$$

$$\begin{cases} v_{dr} = R_r i_{dr} + \frac{d}{dt}\varphi_{dr} - (\omega_s - \omega)\varphi_{qr} \\ v_{qr} = R_r i_{qr} + \frac{d}{dt}\varphi_{qr} + (\omega_s - \omega)\varphi_{dr} \end{cases} \tag{10}$$

where, v_{ds}, $v_{qs,}$ v_{dr},v_{dr} are are characterized as the dq-axis voltage's stator and rotor. R_s and R_r are the resistances of the rotor and stator. φ_{ds}, φ_{qs}, φ_{dr}, and φ_{qr} are demonstrated as the stator and rotor of dq-axis flux. ω and ω_r are the reference rotation speed and the electrical speed. The rotor and stator powers, both active and reactive, are determined by [23]:

$$\begin{cases} P_s = v_{ds} i_{ds} + v_{qs} i_{qs} \\ Q_s = v_{qs} i_{ds} - v_{ds} i_{qs} \end{cases} \tag{11}$$

$$\begin{cases} P_r = v_{dr} i_{dr} + v_{qr} i_{qr} \\ Q_r = v_{qr} i_{dr} - v_{dr} i_{qr} \end{cases} \tag{12}$$

The electromagnetic torque T_{em} is given by [24].

$$T_{em} = p \cdot \frac{M}{L_s}(\varphi_{qs} i_{dr} - \varphi_{ds} i_{qr}) \tag{13}$$

5. CONTROL STRATEGY OF THE DOUBLY FED INDUCTION GENERATOR

5.1. Reactive and active power decoupling

A three-phase setup is necessary when the DFIG is linked to an already existing network. Matching the stator voltages to the network voltages, which act as indicators is the first step. Connecting the stator to this network is the next stage. The link can then be set up after this is finished. Following this connection, the third step is to regulate the power transit between the DFIG and the grid. A stator flux field-oriented method is typically employed to attain high-performance wind system control. Therefore, by setting the stator's quadratic component to the null value as (14) [25].

$$\varphi_s = \varphi_{ds} \quad \Rightarrow \quad \varphi_{qs} = 0 \tag{14}$$

The torque is then made simpler as shown (15)

$$\begin{cases} \varphi_{ds} = L_s i_{ds} + M i_{dr} \\ 0 = L_s i_{qs} + M i_{qr} \end{cases} \tag{15}$$

By omitting the stator resistance R_s,

$$\begin{cases} v_{ds} = 0 \\ v_{qs} = V_s \end{cases} \tag{16}$$

The (17) are acquired by using the aforementioned condition (14) and substituting the rotor flux (15) in (10). The rotor voltages are [26]:

$$\begin{cases} v_{dr} = \sigma L_r \frac{di_{dr}}{dt} + R_r i_{dr} - \sigma L_r \omega_r i_{qr} + \frac{M}{L_s}\frac{d\varphi_{ds}}{dt} \\ v_{qr} = \sigma L_r \frac{di_{qr}}{dt} + R_r i_{qr} + \sigma L_r \omega_r i_{dr} + \frac{M}{L_s}\omega_r \varphi_{ds} \end{cases} \tag{17}$$

where: $\omega_r = \omega_s - \omega = g\omega_s$ is the slip frequency, g is the slip range and $\sigma = 1 - \frac{M^2}{L_s L_r}$ is the leakage coefficient. The rotor voltages can be rewritten as [27]:

$$\begin{cases} v_{dr} = \sigma L_r \frac{di_{dr}}{dt} + R_r i_{dr} + f_{em,d} \\ v_{qr} = \sigma L_r \frac{di_{qr}}{dt} + R_r i_{qr} + f_{em,q} \end{cases} \tag{18}$$

with $f_{em,d}$ and $f_{em,q}$ are the coupling terms between the crosses d-axis and q-axis:

$$\begin{cases} f_{em,d} = -\sigma L_r \omega_r i_{qr} + \frac{M}{L_s} \cdot \frac{d\varphi_{ds}}{dt} \\ f_{em,q} = -\sigma L_r \omega_r i_{dr} + \frac{M}{L_s} \cdot \omega_r \cdot \varphi_{ds} \end{cases} \tag{19}$$

These rotor currents are the only way to express the stator's active and reactive power [21]:

$$\begin{cases} P_s = V_s i_{qs} = -V_s \frac{M}{L_s} i_{qr} \\ Q_s = V_s i_{ds} = \frac{V_s \varphi_s}{L_s} - \frac{V_s M}{L_s} i_{dr} \end{cases} \tag{20}$$

5.2. Super twisting sliding mode control control design

STSMC is a powerful method used to address the issue of chattering present in traditional SMC, while retaining the benefits of robustness and finite-time convergence. The design involves a continuous control action whose time derivative is discontinuous, essentially acting on the second-order dynamics of the sliding variable.

The powers' errors are as (21):

$$\begin{cases} S_c(P) = (P_s^* - P_s) \\ S_c(Q) = (Q_s^* - Q_s) \end{cases} \tag{21}$$

where P_s^* and Q_s^* are the reference values for the stator's active and reactive power. Next up, we will have:

$$\begin{cases} \dot{S}_c(P) = \left(\dot{P}_s^* - \dot{P}_s\right) \\ \dot{S}_c(Q) = \left(\dot{Q}_s^* - \dot{Q}_s\right) \end{cases} \quad (22)$$

Changing (21) into (22) leads to (23).

$$\begin{cases} \dot{S}_c(P) = \left(\dot{P}_s^* + V_s \frac{MR_r}{L_s\sigma L_r}\left(\frac{1}{R_r}v_{rq} - i_{qr} - \frac{\sigma L_r \omega_r}{R_r} i_{dr} - gM\frac{V_s}{R_r.L_s}\right)\right) \\ \dot{S}_c(Q) = \left(\dot{Q}_s^* + V_s \frac{M\cdot R_r}{L_s\sigma L_r}\left(\frac{1}{R_r}v_{dr} - i_{dr} - \frac{\sigma L_r}{R_r}\omega_r i_{qr}\right)\right) \end{cases} \quad (23)$$

Thus, the corresponding command is provided by (24).

$$v_{qr,eq} = R_r i_{qr} + \sigma L_r \omega_r i_{dr} + g\frac{MV_s}{L_s} + i_{qr}\frac{MV_s}{L_s} \quad (24)$$

Therefore:

$$v_{qr}^n = -\lambda_1 |S_c(P)|^{\rho} sign\left(S_c(P)\right) - \beta_1 \int sign\left(S_c(P)\right) dt \quad (25)$$

The correspondent command is is $v_{dr,eq}$ is defined as (24).

$$v_{dr,eq} = -\frac{\sigma L_s}{M}\left(R_r i_{qr} + \dot{\phi}_s - \lambda M i_{dr} - \frac{MR_r}{\sigma L_r} i_{dr} + M\omega_r i_{qr}\right) \quad (26)$$

Therefore:

$$v_{dr}^n = -\lambda_1 |S_c(Q)|^{\rho} sign\left(S_c(Q)\right) - \beta_1 \int sign\left(S_c(Q)\right) dt \quad (27)$$

5.3. Fractional-order super twisting algorithm design

In the following study, the primary objective is to apply the FOSTA to the DFIG, which is described in this section. The requirement that the derivative of the sliding surfaces is zero $S_{dq} = 0$ is applied in order to obtain the whole rotor control voltage vector v_{dr} and v_{qr}. In the absence of disturbances, the equivalent control vector u_{dqeq}, which is the ideal control effort required in order to keep the system moving on the sliding surface, is produced in this stage. The following relation, which is obtained by setting the sliding surface equation's time derivative to zero, typically provides the corresponding control components:

$$u_{eq,dq} = \begin{bmatrix} \left(-\frac{\sigma L_s L_r}{V_s M}\left(R_r i_{qr} + \sigma L_r \omega_r i_{dr} + \frac{gM}{L_s}V_s\right) - \lambda\frac{\sigma L_s L_r}{V_s M}\left(\frac{V_s \varphi}{L_s} - \frac{V_s M}{L_s} i_{dr}\right)\right) \\ \left(-\frac{\sigma L_s L_r}{V_s M}\left(R_r i_{dr} - \sigma L_r \omega_r i_{qr}\right) - \lambda\frac{\sigma L_s L_r}{V_s M}\left(R_r i_{dr} + \sigma L_r \omega_r i_{qr} + \frac{gM}{L_s}V_s\right)\right) \end{bmatrix} \quad (28)$$

$$\begin{cases} u_{ST} = [u_1 + u_2]^{\gamma} \\ \dot{u}_1 = \rightleftarrows -\lambda sign(S) \\ u_2 = -\alpha |s|^{\frac{1}{2}} sign(S) \end{cases} \quad (29)$$

where: $\alpha > 0, \lambda > 0\ \gamma \neq 0$

6. RESULTS AND DISCUSSION

The FOSTA evaluation employs a rigorous simulation methodology to compare its performance against traditional control methods. This structured approach ensures the reliability and reproducibility of results concerning system resilience and tracking efficacy. Methodology and configuration:

– Test condition: to thoroughly evaluate the FOSTA's resilience and efficacy, a comparative analysis will be carried out in situations with fluctuating wind speeds.
– System model: a wind turbine with 7.5 kW with a DFIG is used in the simulation.
– Simulation environment: MATLAB/Simulink is used to build the system model.
– Parameters: Table 1 lists the precise parameter settings for the DFIG that was utilized in the simulation.
– Tracking performance: when compared to the traditional STA-based system, the FOSTA-based system obtains almost the same tracking performance for the DFIG stator powers.

– Chattering effect: there is a notable chattering effect in the classical (traditional) sliding mode control scheme.
– FOSTA advantage: there is no chattering in the FOSTA-based system. The FOSTA delivers great tracking performance and is eventually regarded superior than the standard STSMC because to its ability to minimize chattering.

The efficacy of the proposed FOSTA relative to the traditional STA is visually confirmed by observing the generator's power control responses under the simulated conditions. Figure 4 illustrates the power control characteristics of the DFIG when governed by the conventional STA scheme, showing how effectively the reference power is tracked, but also revealing inherent control limitations. In contrast, Figure 5 provides the corresponding power control results for the same DFIG system when the advanced FOSTA is implemented, allowing for a direct comparison of the two control methodologies, particularly regarding chattering mitigation and steady-state performance.

Table 1. The parameter

Component	Rated power/voltage/number of pole pairs	Stator electrical parameters	Rotor electrical parameters
DFIG nominal parameters	7.55 kW	$M = 0.078\ H$	$50\ Hz$
	$p = 2$	$R_s = 0.455\ \Omega$	$R_r = 0.62\ \Omega$
	380/660 V	$L_s = 0.084\ H$	$L_r = 0.081\ H$
Turbine parameters		Blade configuration	
	Diameter = 13 m		Number of blades = 3
(DFIG+turbine) parameters	Total moment of inertia		Viscous friction coefficient
	$J = 0.3125\ kg \cdot m^2$		$f = 0.00673\ kg \cdot m^2/s$

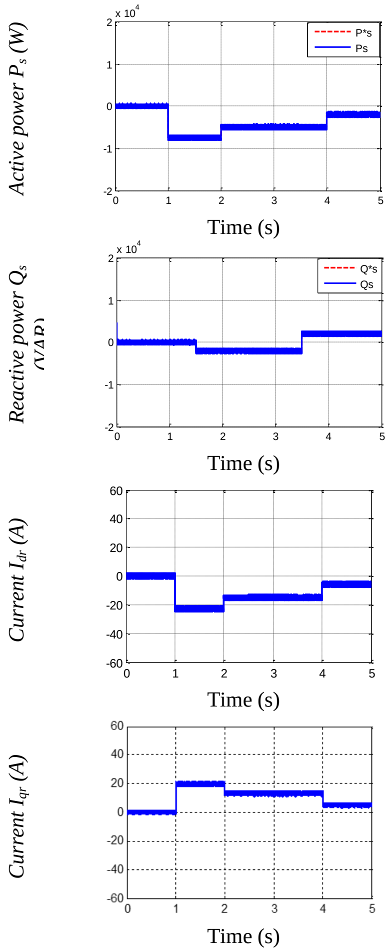

Figure 4. Power control of the DFIG with STA

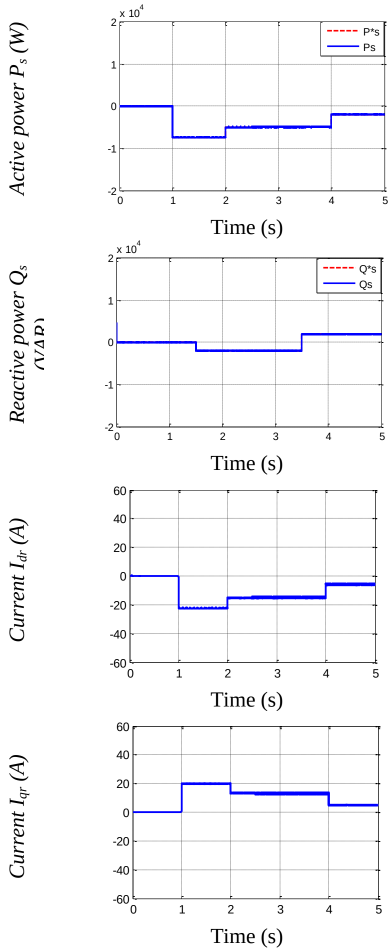

Figure 5. Power control of the DFIG with FOSTA

The controller parameters utilized for both the STA and FOSTA algorithms, which are essential for study reproducibility, are itemized below in Table 2. The performances of the three controllers are shown in Tables 3 and 4. Where $t_{r5\%}$ is the system's reaction time, reject is the amount of time needed for the power to reach the reference-defined corridor during the same test, and ΔX reject is the greatest discrepancy, in the case of a disturbance, between the measured power (active and reactive) and the reference power.

Table 2. Controller parameters

Parameter	Physical effect	Data
α	Governs reaching phase dynamics	12
λ	Rejects steady-state disturbances	25
γ	Accelerates convergence near $S = 0$	0.02

Table 3. Performance comparison of FOSTA, SMC, and STA active power regulators

Active power regulator	$t_{r5\%}$ (ms)	ΔX (W)	t_{rejet} (ms)
SMC	135	320	150
STA	98	130	45
FOSTA	20	45	21

Table 4. Performance comparison of FOSTA, SMC, and STA reactive power regulators

Reactive power regulator	$t_{r5\%}$ (ms)	ΔX (W)	t_{rejet} (ms)
SMC	138	340	135
STA	53	140	35
FOSTA	19	30	15

7. CONCLUSION

In the study, we have shown a full energy-production system using a DFIG-based wind turbine. A DFIG with two converters linking the rotor to the same network is the system under investigation (machine inverter, and grid inverter). Machine control was used to manage the flow of both active and reactive electricity between the machine and the grid. Three different controllers are synthesized and compared. In relation to reference tracking, disturbance susceptibility, and parameter changes. The established technique has solved the main limitations of FOSTA, such as the large reactive and active power changes caused by the switching frequency. Furthermore, oscillations of active and reactive power have been improved. Simplicity, ease of implementation, great robustness, and exceptional proficiency in improving system features characterize the designed command. Following the presentation of the turbine and DFIG mathematical models, the planned method was examined, during which the underlying principle of operation was explained and the required equations were provided. The anticipated technique was then put into practice using MATLAB. When compared to the STA regulator, the results demonstrated the FOSTA's great competency by minimizing the rates of undulations and overshoot. The dynamic attributes (torque, reactive power, and active power) showed a significant improvement, according to the numerical data.

FUNDING INFORMATION

Authors state no funding involved.

AUTHOR CONTRIBUTIONS STATEMENT

This journal uses the Contributor Roles Taxonomy (CRediT) to recognize individual author contributions, reduce authorship disputes, and facilitate collaboration.

Name of Author	C	M	So	Va	Fo	I	R	D	O	E	Vi	Su	P	Fu
Kheira Belgacem	✓	✓	✓	✓	✓	✓	✓	✓	✓	✓		✓	✓	
Houaria Abdelli	✓		✓		✓		✓		✓	✓	✓			
Mebarka Atig		✓		✓			✓	✓	✓			✓	✓	
Abdelkader Mezouar		✓			✓		✓	✓		✓	✓	✓	✓	✓

C : **C**onceptualization
M : **M**ethodology
So : **So**ftware
Va : **Va**lidation
Fo : **Fo**rmal analysis
I : **I**nvestigation
R : **R**esources
D : **D**ata Curation
O : Writing - **O**riginal Draft
E : Writing - Review & **E**diting
Vi : **Vi**sualization
Su : **Su**pervision
P : **P**roject administration
Fu : **Fu**nding acquisition

CONFLICT OF INTEREST STATEMENT

Authors state no conflict of interest.

DATA AVAILABILITY

The data that support the findings of this study are available on request from the corresponding author [Belgacem Kheira]. The data, which contain information that could compromise the privacy of research participants, are not publicly available due to certain restrictions. Derived data supporting the findings of this study are available from the corresponding author [Belgacem Kheira] on request.

REFERENCES

[1] M. M. Baggu, B. H. Chowdhury, and J. W. Kimball, "Comparison of advanced control techniques for grid side converter of doubly-fed induction generator back-to-back converters to improve power quality performance during unbalanced voltage dips," *IEEE Journal of Emerging and Selected Topics in Power Electronics*, vol. 3, no. 2, pp. 516–524, Jun. 2015, doi: 10.1109/JESTPE.2014.2359205.

[2] A. A. Chhipą *et al.*, "Modeling and control strategy of wind energy conversion system with grid-connected doubly-fed induction generator," *Energies*, vol. 15, no. 18, p. 6694, Sep. 2022, doi: 10.3390/en15186694.

[3] F. Mesa, G. C. Vélez, and J. J. B. Ortega, "Stability by assigning structures by applying the multivariable subspace identification algorithm for a wind system with a DFIG," *TELKOMNIKA Telecommunication Computing Electronics and Control* Vol. 21, No. 4, Aug. 2023, pp. 901-908, doi: 10.12928/telkomnika.v21i4.24431.

[4] N. El Ouanjli *et al.*, "Direct torque control of doubly fed induction motor using three-level NPC inverter," *Protection and Control of Modern Power Systems*, vol. 4, no. 3, pp. 1–9, Jul. 2019, doi: 10.1186/s41601-019-0131-7.

[5] A. Herizi, R. Rouabhi, F. Ouagueni, and A. Zemmit, "Robust wind power control using sliding mode, backstepping, and fuzzy logic," *Dynamics*, vol.70, 3, pp. 313–318, 2025.

[6] K. Belgacem, A. Mezouar, and A. Massoum, "Fuzzy logic control of double-fed induction generator wind turbine," *International Review on Modelling and Simulations*, Jun. 2008.

[7] H. Abdelli, A. Mezouar, M. Bendjebbar, and K. Belgacem, "Synthesis of smc algorithms applied to wind generator," *International Journal of Power Electronics and Drive Systems (IJPEDS)*, vol. 12, no. 1, pp. 404–412, Mar. 2021, doi: 10.11591/ijpeds.v12.i1.pp404-412.

[8] H. Benbouhenni, N. Bizon, I. Colak, P. Thounthong, and N. Takorabet, "Simplified super twisting sliding mode approaches of the double-powered induction generator-based multi-rotor wind turbine system," *Sustainability (Switzerland)*, vol. 14, no. 9, p. 5014, Apr. 2022, doi: 10.3390/su14095014.

[9] Z. Song and W. Zhou, "PMSM disturbance resistant adaptive fast super-twisting algorithm speed control method," *IEEE Access*, vol. 12, pp. 138155–138165, 2024, doi: 10.1109/ACCESS.2024.3467050.

[10] I. González-Hernández, S. Salazar, R. Lozano, and O. Ramírez-Ayala, "Real-time improvement of a trajectory-tracking control based on super-twisting algorithm for a quadrotor aircraft," *Drones*, vol. 6, no. 2, p. 36, Jan. 2022, doi: 10.3390/drones6020036.

[11] F. Echiheb *et al*., "Robust sliding-Backstepping mode control of a wind system based on the DFIG generator," *Scientific Reports*, vol. 12, no. 1, July 2022, doi: 10.1038/s41598-022-15960-7.

[12] V. Q. Leu, H. H. Choi, and J. W. Jung, "Fuzzy sliding mode speed controller for PM synchronous motors with a load torque observer," *IEEE Transactions on Power Electronics*, vol. 27, no. 3, pp. 1530–1539, Mar. 2012, doi: 10.1109/TPEL.2011.2161488.

[13] H. Gasmi, S. Mendaci, S. Laifa, W. Kantas, and H. Benbouhenni, "Fractional-order proportional-integral super twisting sliding mode controller for wind energy conversion system equipped with doubly fed induction generator," *Journal of Power Electronics*, vol. 22, no. 8, pp. 1357–1373, Aug. 2022, doi: 10.1007/s43236-022-00430-0.

[14] M. Maaruf and M. Khalid, "Global sliding-mode control with fractional-order terms for the robust optimal operation of a hybrid renewable microgrid with battery energy storage," *Electronics (Switzerland)*, vol. 11, no. 1, p. 88, Dec. 2022, doi: 10.3390/electronics11010088.

[15] G. Li, B. Chen, H. Chen, and W. Deng, "Fractional-order PIλDμ controller using adaptive neural fuzzy model for course control of underactuated ships," *Applied Sciences (Switzerland)*, vol. 12, no. 11, p. 5604, May 2022, doi: 10.3390/app12115604.

[16] S. M. Alwash, O. Q. J. Al-Thahab, and S. F. Alwash, "Modeling and control strategies for DFIG in wind turbines: A Comparative Analysis of SPWM, THIPWM, and SVPWM Techniques," *JESA*, vol. 56, no. 6, pp. 963–972, Dec. 2023, doi: 10.18280/jesa.560607.

[17] S. P. Mohapatra and P. K. Dash, "A novel control strategy of a variable-speed doubly-fed-induction-generator-based wind energy conversion system," *Clean Energy*, vol. 8, no. 1, pp. 153–170, Jan. 2024, doi: 10.1093/ce/zkad074.

[18] S. Kadi, K. Imarazene, E. M. Berkouk, H. Benbouhenni, and E. Abdelkarim, "A direct vector control based on modified SMC theory to control the double-powered induction generator-based variable-speed contra-rotating wind turbine systems," *Energy Reports*, vol. 8, pp. 15057–15066, Nov. 2022, doi: 10.1016/j.egyr.2022.11.052.

[19] R. Errouissi, A. Al-Durra, S. M. Muyeen, S. Leng, and F. Blaabjerg, "Offset-free direct power control of DFIG under continuous-time model predictive control," *IEEE Transactions on Power Electronics*, vol. 32, no. 3, pp. 2265–2277, Mar. 2017, doi: 10.1109/TPEL.2016.2557964.

[20] A. Merabet , H. Eshaft, A. A. Tanvir "Power-current controller based sliding modecontrol for DFIG-wind energy conversion system" *IET Renewable Power Generation*, 2018, Vol. 12 Iss. 10, pp. 1155-1163, doi: 10.1049/iet-rpg.2017.0313.

[21] A. Sobhy, M. H. Elfar, A. Refaat, and M. Fawzi "Performance evaluation of an optimized simplified nonlinear active disturbance rejection controller for rotor current control of DFIG-based wind energy system," *Cleaner Engineering and Technology*, vol. 24, p. 100896, Feb. 2025, doi: 10.1016/j.clet.2025.100896.

[22] E. Bekiroglu and M. D. Yazar, "MPPT control of grid connected DFIG at variable wind speed," *Energies*, vol. 15, no. 9, p. 3146, Apr. 2022, doi: 10.3390/en15093146.

[23] M. Guediri *et al*., "Control of a doubly fed induction generator for variable speed wind energy conversion systems using fuzzy controllers optimized with a genetic algorithm," *Engineering, Technology & Applied Science Research*, vol. 15, no. 1, pp. 19871–19877, Feb. 2025, doi: 10.48084/etasr.9460.

[24] T. Ghennam, E. Berkouk, and B. Francois, "A vector hysteresis current control applied on three-level inverter. application to the active and reactive power control of doubly fed induction generator based wind turbine," *International Review of Electrical Engineering*, 2007.
[25] L. Qi, W. jiahui , W. Haiyun, Z. Hua, and Y. Jian, "Effect of DFIG control parameters on small signal stability in power systems," *Scientific Report*, vol. 13, no. 1, Feb. 2023, doi: 10.1038/s41598-023-29278-5.
[26] O. E. M. Youssef, M. G. Hussien, and A. E.-W. Hassan, "An advanced control performance of a sophisticated stand-alone wind-driven DFIG system," *International Transactions on Electrical Energy Systems*, vol. 2023, pp. 1–11, Aug. 2023, doi: 10.1155/2023/5541932.
[27] Z. Chen, T. Shi, Z. Lin, Z. Wang, and X. Gu, "Analysis and control of current harmonic in IPMSM field-oriented control system," *IEEE Transactions on Power Electronics*, vol. 37, no. 8, pp. 9571–9585, Aug. 2022, doi: 10.1109/TPEL.2022.3155243.

BIOGRAPHIES OF AUTHORS

Kheira Belgacem received B.S. degree in Electrical Engineering from Taher Moulay University, Saida, Algeria, in 2001 and the M.S. degree from High National Schools of Technical Studies (ENSET) in 2009. Subsequently, she received the Ph.D. degree from DjillaliLiabes University, Sidi Bel Abbès, Algeria, in 2014. She is currently a member of the Laboratory of Electrical Engineering, Taher Moulay University, Saida, Algeria. His research interests include electrical machines and drives, sliding mode control, modelling and control of wind turbines, and renewable energy. She can be contacted at email: kheira.belgacem@yahoo.fr.

Houaria Abdelli is Ph.D. student in the Department of Electrical Engineering at the University of Sciences and Technology (USTO-MB) of Oran, Algeria. She received Magister degree in Industrial Control of Electrical Drives and Diagnosis from the University of Science and Technology of Oran (USTO-MB), Algeria in 2011. Her major research interests are modeling, control of electrical machines and control of wind turbine. She can be contacted at email: abdelli_houaria@yahoo.com.

Mebarka Atig is Ph.D. student in the Department of Electrical Engineering at the University Dr Moulay Tahar of Saida, Algeria. She received Magister degree in Industrial Control of Electrical Drives and Diagnosis from the University of Science and Technology of Oran (USTO-MB), Algeria in 2011. His main research interests revolve around renewable energy concerning photovoltaic. She can be contacted at email: at_m74@yahoo.com.

Abdelkader Mezouar received the B.S. and M.S. degrees in Electrical Engineering from National Polytechnic School, Algiers, Algeria, in 1997 and 1999 respectively. Subsequently, he received the Ph.D. degree and the University Habilitation from DjillaliLiabes University, Sidi Bel Abbès, Algeria, in 2006 and 2008 respectively. He is currently the president of the Laboratory of Electrical Engineering, Taher Moulay University, Saida, Algeria. His research interests include electrical machines and drives, sliding mode control, observer techniques and renewable energy. He can be contacted at email: a.mezouar@yahoo.fr.